

Collisions of trapped ions with ultracold atoms in the $[\text{YbRb}]^+$ system

H. D. L. Lamb* and J. F. McCann†

Centre for Theoretical Atomic, Molecular and Optical Physics, School of Mathematics and Physics,
Queen's University Belfast, Belfast BT7 1NN, Northern Ireland, UK

J. Goold

Clarendon Laboratory, University of Oxford, United Kingdom,
Department of Physics, University College Cork, Ireland

N. Wells and I. Lane

Innovative Molecular Materials Group, School of Chemistry and Chemical Engineering,
Queen's University Belfast, Belfast BT7 1NN, Northern Ireland, UK

(Dated: July 7, 2011)

We investigate the ultracold elastic scattering for the quasi-molecular ion of ytterbium and rubidium system, based on *ab initio* calculations, including both asymptotic ionic channels. This structure has an important role in the design of hybrid ion-atom traps and quantum control of charge transfer processes. The dissociation energies and molecular constants for the lowest electronic states were calculated along with the long-range dispersion forces in order to estimate the scattering lengths. The separated-atom ionization potentials and atomic polarizability of the ytterbium atom ($\alpha_d = 128.5$ atomic units) are in good agreement with experiment and previous calculations. Using phase shift analysis and the semiclassical approximation, for the Rb^+ channel the scattering length is $a_s \approx +2815 a_0$. With the Yb^+ ion colliding with the Rb atom we have the complications of singlet/triplet and the presence of nearly-degenerate charge transfer states introducing uncertainty. For the triplet channel, the adiabatic scattering length is estimated at $a_s \approx -680 a_0$, while the singlet value is $a_s \approx -690 a_0$. We also find that the pseudopotential has a strong linear variation near zero energy and is not well represented by the single-parameter scattering length. Thus, for calculations of scattering processes at low (μK) temperatures it is essential to take this variation into account.

I. INTRODUCTION

As a gas is cooled to towards micro-Kelvin temperatures the quantum nature of the interactions begins to dominate. With increasing de Broglie wavelength, the long-range tail of the potential plays a key role in determining the nature of the interactions. In particular whether the elastic pair-wise interaction is, in the limit of zero temperature, attractive or repulsive [1, 2]. The lower the incident energy of the ion-atom pair, the larger the distances for which these potentials influence the phase shift. This is critical in terms of the ultracold regime as to whether cooling, trapping and degeneracy can occur. It is extremely important in view of potential applications [3–5].

Interest has developed in expanding the range of quantum systems that can be trapped and manipulated on the quantum scale. Hybrid ion-atom systems are of great interest [6]. Recently these systems have been explored considering two-body collisions, in which both collision partners are translationally cold [7], and on the many-body level [8], where the sympathetic cooling of the ion with ultracold atoms was observed. The study of these systems in the quantum regime can be applied to hy-

brid atom-ion devices [9] and, in addressing fundamental many-body effects of ionic impurities such as mesoscopic molecule formation [10] and density fluctuations [11].

Ultracold neutral atom interactions are characterised by pure *s*-wave scattering mediated at long-range by the dispersion forces [12]. Conversely, a bare ion creates a polarization force directly and hence the effective cross section is larger with significant contributions from higher-order partial waves [13]. Indeed the usual effective range expansion is modified by logarithmic terms in the wavenumber expansion [14]. In the last few years theoretical studies of ultracold atom-ion collisions included the investigation of the occurrence of magnetic Feshbach resonances with a view to examining the tunability the atom-ion interaction focusing on the specific ${}^{40}\text{Ca}^+ + \text{Na}$ system [15], and calculations of the single-channel scattering properties of the Ba^+ ion with the Rb neutral atom [16] which suggest the possibility of sympathetic cooling of the barium ion by the buffer gas of ultracold rubidium atoms with a considerable efficiency.

In recent experiments [7, 8, 17], a single trapped ion of ${}^{174}\text{Yb}^+$ in a Paul trap was immersed in a condensate of neutral ${}^{87}\text{Rb}$ atoms confined in a magneto-optical trap. However, little known about the microscopic ultracold binary interactions between this ion and the rubidium atom. In particular, the scattering length is not known with any great accuracy thus prompting our in depth investigations. Our initial aim was to determine the static properties of the molecular ion, the dissociation

*Electronic address: hlamb01@qub.ac.uk.

†Electronic address: j.f.mccann@qub.ac.uk

energies and molecular constants, along with the electronic energy surfaces. Using this information we have obtained parameters for the pseudo-potential which approximates the ultracold interaction. This information is of great importance for modelling a variety of phenomena, synonymous with many-body physics, in the framework of second quantisation. It is also of great interest for laser manipulation of the collision to prevent losses through charge transfer or create translationally-cold trapped molecular ions via photoassociation.

II. ELECTRONIC STRUCTURE CALCULATION

Our *ab initio* data points are calculated using effective core potentials (ECP) as a basis set for each atom. A multi-configuration self-consistent field (MCSCF) calculation was performed on the lowest five electronic states, and the results used as the initial wavefunction set for a multi-reference configuration interaction (MRCI) calculation to capture the dynamic electron correlation. The short-range interactions for the molecular electronic states used the non-relativistic CASSCF/MRCI method [18–21] within the MOLPRO [22] *ab initio* suite (release MOLPRO 2010.1). The inner shell effect were modeled using effective core potentials ECP68MDF for ytterbium [23], and ECP36SDF for rubidium [24, 25] were used. Only the valence shells were included in the determination of the electronic correlation energy. As a test of the basis set employed, we conducted equivalent calculations of the neutral YbRb molecule and our results were in excellent agreement with those of Meyer and Bohn [26].

One of the more challenging tasks for a quantum chemistry package is the calculation of polarizabilities and dispersion forces at long-range which of course is essential to scattering calculations [27]. Asymptotically the ion-atom potential has the form [12, 13]

$$V(r) = -\frac{1}{2} \left[\frac{\alpha_d}{R^4} + \frac{C_6}{R^6} + \frac{C_8}{R^8} \right], \quad (1)$$

where C_6 and C_8 are respectively the quadrupole and octupole polarizabilities. Thus, the leading-order multipole of the (singly-charged) ion-atom potential has the well-known form:

$$V(R) \sim -\frac{\alpha_d}{2R^4}, \quad (2)$$

where α_d is the dipole polarizability of the neutral atom, and we use atomic units. A recent review of existing theoretical methods for polarizability discusses their relevance to cold-atom physics [27]. Calculations of polarizability for molecules with heavy atoms become increasingly difficult, partly because of relativistic corrections, but in the case of Rb electron correlation is the primary problem. For example, a simple non-relativistic Hartree-Fock calculation [28] gives $\alpha_d \approx 522$ (atomic units), and

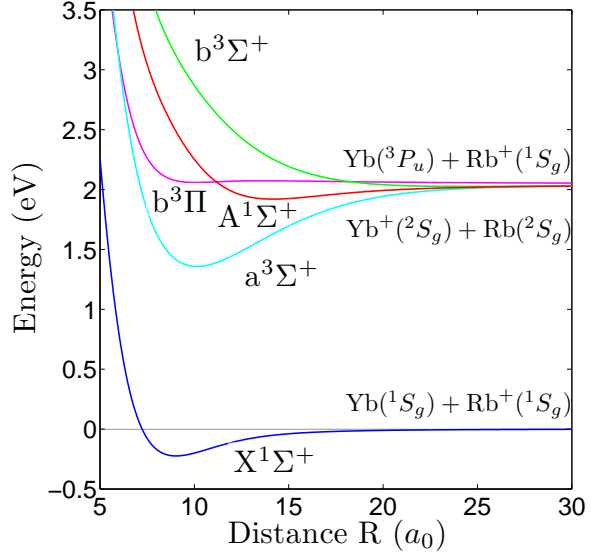


FIG. 1: Electronic energies for the molecular ion $[\text{YbRb}]^+$. The $X^1\Sigma^+$ ground state is the Rb^+ channel, while the lowest energy ionic ytterbium states, the triplet $a^3\Sigma^+$ and singlet $A^1\Sigma^+$ pair, are nearly degenerate with the excited charge-transfer channels: $\text{Rb}^+ + \text{Yb}^*$.

it requires the power of the coupled-cluster expansions to account fully for correlation. The CCSD(T) method gives [28] $\alpha_d \approx 352$ (a.u.) (non-relativistic), while it takes relativistic corrections to yield, $\alpha_d \approx 324$ (a.u.) which is consistent with experiment: 319 ± 6 [29].

The spin-orbit splitting is absent since the MRCI calculations do not include relativistic effects. This is not important for the entrance collision channel or the lower $\text{Yb}^+(1S) + \text{Rb}^+(1S)$ asymptote as all the molecular states formed are of Σ^+ symmetry. This is borne out by the calculated energy of the asymptotic energies of the $a^3\Sigma^+$ and $A^1\Sigma^+$ states (Table I).

The asymptotes for the higher $^3\Pi$ and $^3\Sigma$ states correlate to the $\text{Yb}^+(^3P_0) + \text{Rb}^+(^1S)$ atomic products. The fine-structure splitting in the $\text{Yb}^+(^3P)$ is considerable and only a fully relativistic treatment can accurately account for the spin-orbit splitting. This being said, we can identify that a curve crossing will take place between the $A^1\Sigma^+$ and $^3\Pi$ states though at an energy above the $\text{Yb}^+(^1S) + \text{Rb}^+(^1S)$ asymptote. Such a crossing will facilitate a charge exchange reaction as observed in experiment at mK temperatures [7, 8]. Molecular constants were then determined for the calculated bound potentials using the LEVEL [30] program (version 8.0) and are presented in Table II.

TABLE I: Comparison between the experimental and calculated molecular asymptotes

Molecular Symmetry	Calculated Asymptotic Limit (eV)	Experimental Asymptotic Limit (eV)	Difference (eV)	Difference (%)
$X^1\Sigma^+$	0	0	0	-
$a^3\Sigma^+$	2.036	2.077	0.041	1.97
$A^1\Sigma^+$	2.036	2.077	0.041	1.97
$^3\Pi$	2.045	2.143	0.089	4.15
$^3\Sigma^+$	2.050	2.143	0.093	4.34

TABLE II: Molecular parameters for the calculated states derived from the ab initio data. Equilibrium bond length R_e is in atomic units, vibrational constants ω_e and ω_{exe} , and rotation constants B_e and D_e are in cm^{-1} , and dissociation energy D_e is in eV. The $2^{\text{nd}} \ ^3\Sigma^+$ state is repulsive.

Molecular Symmetry	R_e	ω_e	ω_{exe}	B_e	$D_e(10^{-9})$	D_e
$X^1\Sigma^+$	9.031	33.77	-0.22	0.01273	7.0047	0.2202
$a^3\Sigma^+$	10.142	34.94	0.04	0.01010	3.3843	0.6653
$A^1\Sigma^+$	14.362	16.807	0.38	0.00505	2.1440	0.1085
$^3\Pi$	10.108	15.24	-0.21	0.001015	16.812	0.0061

A. Scattering length calculation

We describe the ion-atom collisions with the radial Schrödinger equation (in atomic units),

$$\left[\frac{d^2}{dR^2} + k^2 - 2\mu V(R) - \frac{J(J+1)}{R^2} \right] \chi_J(k, R) = 0 \quad (3)$$

Here, $k = \sqrt{2\mu E}$ with $\mu = m_i m_a / (m_i + m_a)$ denoting the reduced mass and E the collision energy in the center-of-mass system. The ion and atom masses are denoted by m_i and m_a , respectively. The phase shift δ_J has its usual definition,

$$\chi_J(k, R) \sim \sin \left(kR - \frac{J\pi}{2} + \delta_J(k) \right), \quad R \rightarrow \infty. \quad (4)$$

For a potential of the form (2) we have the effective range expansion for the s -wave [14],

$$\begin{aligned} k \cot \delta_0(k) = & -\frac{1}{a_s} + \frac{\pi \mu \alpha_d}{3a_s^2} k \\ & + \frac{4\mu \alpha_d}{3a_s} k^2 \ln \left(\frac{k}{4} \sqrt{\mu \alpha_d} \right) + \mathcal{O}(k^2) \end{aligned} \quad (5)$$

which defines the s -wave scattering length: a_s . That is,

$$a_s = \lim_{k \rightarrow 0} -\frac{\tan \delta_0(k)}{k}. \quad (6)$$

We note the linear and logarithmic terms in k on the right-hand side of (5) compared with the usual quadratic term for a short-range force. The significance of the scattering length for ultracold gases is as a strength parameter of a pseudo-potential that can, in turn, be used in the many-body Hamiltonian,

$$V(\vec{r}) = \frac{2\pi \hbar^2}{\mu} a_s \delta(\vec{r}) \frac{\partial}{\partial r} \cdot r. \quad (7)$$

B. Semiclassical method

At distances near the equilibrium bond length, R_e , the interaction between the ion charge and the dipole moment in the atom results in a deep potential well for which the thermal de Broglie wavelength, λ , is small, and the potential slowly-varying so that the semiclassical approximation is satisfied. At long range, where the dipole potential is the dominant term, equation (3) can be solved in closed analytic form. Connecting the exact asymptotic solution with the semiclassical approximation at a *matching distance* (R_c) gives the phase shift in terms of a simple quadrature [31, 32]. This, in turn, yields an elegant and simple expression for the scattering length,

$$a_s = -\sqrt{\mu \alpha_d} \tan \left(\Phi - \frac{\pi}{4} \right) \quad (8)$$

where

$$\Phi = \int_{R_0}^{\infty} \sqrt{-2\mu V(R)} dR \quad (9)$$

with R_0 the zero-energy classical turning point i.e. the smallest value for the solution of, $V(R_0) = 0$. The phase (9) is the accumulation of the inner (semiclassical) phase as far as the matching radius, R_c , and the outer (asymptotic) phase beyond the matching radius in the region where the exact solution applies. This can be simply written as [31, 32]: $\Phi = \Phi_{<} + \Phi_{>}$, where

$$\Phi_{<} = \int_{R_0}^{R_c} \sqrt{-2\mu V(R)} dR, \quad \Phi_{>} = \sqrt{\mu \alpha_d} \frac{1}{R_c}. \quad (10)$$

In accordance with Levinson's theorem, the phase Φ oscillates through many cycles of π at the threshold energy. For a dipole potential of the form (2) and within the

semiclassical approximation, the number of bound states is given by

$$n_s = \text{int} [\Phi/\pi - 3/4] + 1. \quad (11)$$

The large, but uncertain, value of the phase leads one to the conjecture [31] that there is equal likelihood that the scattering length is positive or negative, and indeed it may be infinitely large in magnitude. This sensitivity of scattering length to phase shift, which in turn depends on the interatomic potential amplified by the large reduced mass, means that obtaining accurate and reliable theoretical estimates of the scattering length is extremely difficult. Nonetheless, one of the aims of this paper is to make a first estimate of these values.

III. RESULTS

A. Ground state

Firstly, consider the $X^1\Sigma^+$ electronic potential corresponding to the asymptotic channel, $\text{Rb}^+ (4p^6 \ ^1S_g) + \text{Yb}(6s^2 \ ^1S_g)$. In this case, the ytterbium atom experiences the long range single charge of the the Rb ion, and the electronic potential has the leading order term given by (2). As a test of the accuracy of the electronic energy curve we obtained, we estimated the ytterbium polarizability by curve fitting to (2) at values of $R > 30$ (a.u.). Using a least-squares fit over 15 points using a constant and R^{-4} as independent variables for which we computed the coefficients corresponding respectively to the ionization energy and the polarizability of the atomic species. For the ground electronic state $X^1\Sigma^+$, which corresponds asymptotically to $\text{Rb}^+ (4p^6 \ ^1S_g)$ and neutral $\text{Yb}(6s^2 \ ^1S_g)$, the quadrupole polarizability is small at an internuclear distances beyond 30a.u. and can be neglected. We find an estimate of the polarizability of ytterbium is $\alpha_d \approx 128.5$, and values from other calculations are presented in Table I.

In order to calculate the scattering length, we performed a numerical integration using the Runge-Kutta method along with a numerical quadrature (Simpson's rule) for the semiclassical approximation. The numerical integration was started just to the left of the classical turning point and integrated outwards to fit to the form (4). Examples of the results we obtained are shown in Fig. 2.

We integrate numerically using a simple 4th/5th order Runge-Kutta scheme starting within the classically forbidden region out to the matching radius $R_c \sim 37a_0$, a distance sufficiently far so that the potential is well described by a multipole expansion. The leading-order dipole term with the value $\alpha_d = 128.4894$, gives $n_s = 159$ bound states, and we find a large negative scattering length indicating the presence of a virtual bound state at $E = (2\mu a_s^2)^{-1}$. Our calculated polarizability falls within the range of previous theoretical and experimental results as shown in Table III.

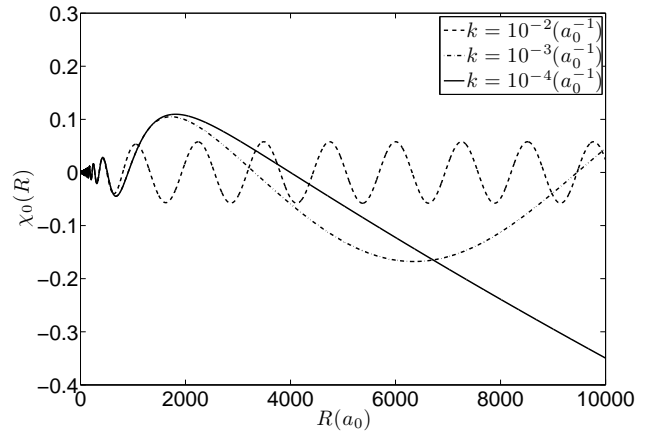


FIG. 2: Low-energy continuum wave functions corresponding to the $X^1\Sigma^+$ molecular potential at sub-mK temperatures ($10 \text{ nK} \lesssim T \lesssim 100 \mu\text{K}$). The scattering length is the outermost intercept of the R axis in the limit $k \rightarrow 0$, in this case 2813.5 a_0 .

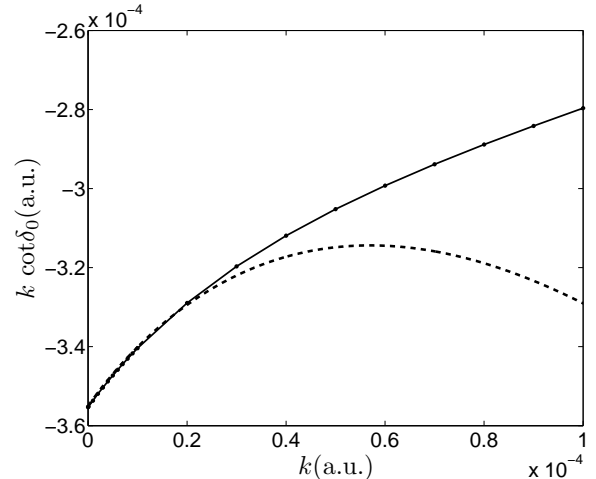


FIG. 3: The effective range function in the limit of low energy. The (numerically) exact function $k \cot \delta_0(k)$ (circles) is compared with the expansion ((5), dashed curve) indicating the nonlinearity, that is deviation from the usual effective range expansion.

In Fig. 2 we show low energy s-wave wave functions. The de Broglie wavelength increases as $k \rightarrow 0$. For $k < 10^{-3}$ ($T \lesssim 1 \mu\text{K}$) the collisional properties are determined by s-wave scattering. We are already well into the nK regime when $k = 10^{-8}$, for which convergence of the phase shift to its value in the low energy limit to reasonable accuracy can be assumed. Integration must be carried out to a distance for which the long ranged dispersion potentials have a negligible effect on the phase, $k^2 \gg \mu \alpha_d / R^4$. The method of extrapolation of the zero-energy wave function is less computationally expensive and can be used as a test against the results for very low energy scattering.

TABLE III: Static electric-dipole polarizability α_d (a.u.) of Yb ($6s^2 \ ^1S_0$) in various approximations.

α_d	Comment
128.5	This work
141(6)	Dzuba and Derivanko; CI+MBPT[33]
136.4(4.0)	Zhang and Dalgarno; based on experimental data, 2007. [34]
157.3	Chu <i>et al</i> ; density functional theory [35]
141(35)	Linear response method ^b , Handbook of Chemistry and Physics, 85 th Ed., 2004-2005

^aRescaling factors are chosen to fit the experimental spectrum of Yb due to such considerations as the mixing of low lying states with equal total angular momentum and parity, and van der Waals interactions. [33]

^bAdjustments of less than 10% across the periodic table have been made to these results to bring them into agreement with accurate experimental values where available. [36]

The numerically obtained low-energy s-wave phase shifts are in good agreement with those from the low-energy phase shift expansion (4) using the semiclassical scattering length $a_{SC} = 2816.7$ in Fig. 3 in the range of $ka_s \lesssim 0.3$, corresponding to temperatures of $T \lesssim 100$ nK.

The variation in the effective potential $a(k) = -\frac{\tan\delta_0}{k}$, using the numerically obtained phase shift, with energy is shown in Fig. 4 below. We also consider comparison with the linear expansion of Eq.(5) , in which case

$$a(k) \approx a_s \left(1 + \frac{\pi\mu\alpha_d}{3a_s} k \right) \quad (12)$$

In Fig. 4 the exact calculation (solid line) deviates both from the linear and log expansions. Evidently, when choosing a fixed value of a_{SC} for the scattering length in (4), omission of the logarithmic correction leads to rapidly increasing errors for even the low energies shown in the graph. The results using the semiclassical method and those from (4) seem to hold to reasonable accuracy for s-wave scattering and are quite close provided $k < 10^{-5}$.)

B. Excited states

In ion trap experiments, the primary interaction will be the $\text{Yb}^+(6s \ ^2S_g)$ ion colliding with the neutral $\text{Rb}(5s \ ^2S_g)$ which may occur in the $A^1\Sigma^+$ singlet or the $a^3\Sigma^+$ triplet state. We see (Fig 1) that the triplet has a lower minimum and shorter bond length, and because of the statistical weight is the more important channel. In the separated-atom limit, this channel lies 2.036eV above the ground state, corresponding to the difference in ionization potentials of Rb and Yb. Considering the long-range numerical values of the potential, we find that the hyperpolarizabilities in the multipole expansion (1) need to be taken into account. Little experimental information about quadrupole or octupole transitions for the heavier

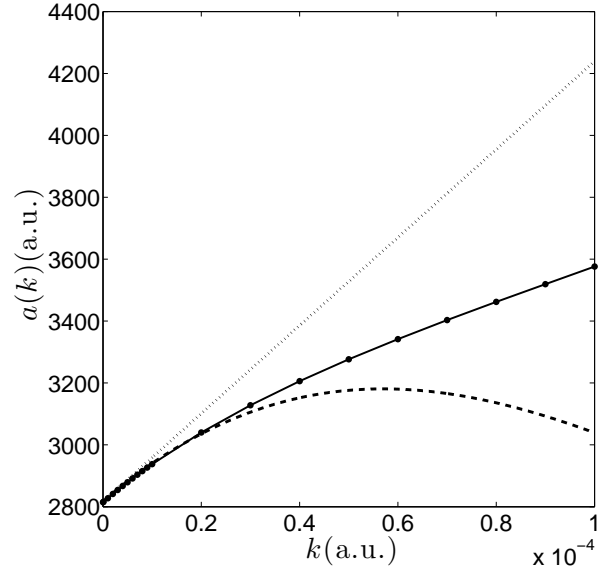


FIG. 4: The effective scattering length for the pseudopotential (7) for the ground state potential curve ($X^1\Sigma^+$). The numerical integration (circles) is shown. The approximate expansion (5) is indicated by the dashed curve, and the linear approximation (12) as a dotted line, with the semiclassical approximation employed for the scattering length. The figure shows that there is considerable variation near zero-energy. The the linear approximation is adequate for $k < 10^{-5}$, while the expansion (5) breaks down above $k = 2 \times 10^{-5}$ as higher order terms become significant.

alkali atoms exists since it is very difficult to measure the oscillator strengths. For the higher-order multipole terms we obtained solutions first by fitting the data to equation (1). In this case, we chose to fix the dipole polarizability by its experimental value 319.2a.u [29] , and then fit the higher-order terms to our data points. This still leaves some flexibility for the fitting procedure. We consider two possible strategies, (a) neglecting C_8 , and then by using the quadrupole polarizability calculated by Mitroy and Bromley [37], and (b) and fitting to obtain C_8 . The results of these two methods and their effect on the scattering length are given in Table IV below.

While these long-range corrections have a negligible effect on the short-range properties such as the bond length and dissociation energy, there are dramatic differences between these methods in terms of the effect on the scattering length.

IV. CONCLUSIONS

We investigated the ultracold elastic scattering for the quasi-molecular ion of ytterbium and rubidium system, based on *ab initio* calculations, including both asymptotic ionic channels. The dissociation energies, molecular constants and long-range dispersion forces were cal-

TABLE IV: $\text{Yb}(6^2S)^+ + \text{Rb}(5^2S)$ states.

Molecular Symmetry	R_c (a_0)	R_e (a_0)	D_e (eV)	C_6 10^5 a.u.	C_8 10^8 a.u.	Asymptote (eV)	a_s (a_0)
$A^1\Sigma^+$	38.465	14.179	0.1162	1.595	-	2.036	65419.9
$A^1\Sigma^+$	36.486	14.179	0.1160	0.06480	1.386	2.036	-686.4
$a^3\Sigma^+$	38.737	10.135	0.6787	1.615	-	2.036	-33013.5
$a^3\Sigma^+$	36.617	10.135	0.6784	0.06480	1.404	2.036	-682.8

culated. The results for the long-range potential tail including the polarizability are in good agreement with experiment and previous work. The calculations for the scattering length indicate strong repulsive interactions in the low-energy limit. We also find that the pseudopotential has a strong linear variation near zero energy and is not well represented by the single parameter scattering length. Thus, for calculations of scattering processes it is essential to take this variation into account. For the Yb^+ ion collisions with Rb, interactions are attractive for both the singlet and triplet.

The sensitivity of scattering length to changes in potential means that these estimates are quite rough. More-

over non-adiabatic effects must have a role to play as well as relativistic corrections. Nonetheless, it is hoped that further experimental and theoretical work will be pursued to understand this complex and interesting system.

Acknowledgments

We are grateful to Dr Brendan McLaughlin for helpful advice and comments. HDLL is grateful to the Department of Employment and Learning (Northern Ireland) for the provision of a postgraduate studentship. J.G. would like to acknowledge funding from an IRCSET Marie Curie International Mobility fellowship.

[1] C. J. Foot. *Atomic Physics*. (2004) OUP.

[2] R. Côté and A. Dalgarno 1998 *Phys. Rev. A* **58**, 498

[3] A. Fioretti *et al.* 1998 *Phys. Rev. Lett.* **80**, 4402

[4] W. C. Swalley and H. Wang 1999 *J. Mol. Spectrosc.* **195**, 194

[5] J. Weiner, V. Bagnato, S. Zilio, and P. S. Julienne 1999 *Rev. Mod. Phys.* **71**, 1 ; G. H. Rawischer, B. D. Esry, E. Tiesinga, J. P. Burke, Jr., I. Koltracht 1999 *J. Chem. Phys.* **111**, 10418

[6] A. T. Grier, M. Cetina, F. Oruevi, and V. Vuleti 2009 *Phys. Rev. Lett.* **102**, 223201 ; W. W. Smith, O. P. Makarov, and J. Lin 2005 *J. Mod. Opt.* **52**, 2253

[7] C. Zipkes, S. Palzer, L. Ratschbacher, C. Sias and M. Köhl 2010 *Phys. Rev. Lett.* **105**, 133201

[8] C. Zipkes, S. Palzer, C. Sias and M. Köhl 2010 *Nat. Lett.* **464** 388

[9] Z. Idziaszek, T. Calarco, and P. Zoller 2007 *Phys. Rev. A* **76**, 033409 (16)

[10] R. Côté, V. Kharchenko, and M. D. Lukin 2002 *Phys. Rev. Lett.* **89**, 093001

[11] J. Goold, H. Doerk, Z. Idziaszek, T. Calarco and T. Busch 2010 *Phys. Rev. A* **81** 041601(R)

[12] J O Hirshfelder, C F Curtiss and R B Bird. *Molecular theory of gases and liquids*. 1954. Wiley (New York).

[13] R. Côté and A. Dalgarno 2000 *Phys. Rev. A* **62** 012709

[14] T. F. O'Malley, L. Spruch and L. Rosenberg 1961 *J. Math. Phys.* **2** 491

[15] Z. Idziaszek, T. Calarco, P. S. Julienne and A. Simoni 2009 *Phys. Rev. A* **79**, 010702(R)

[16] M. Krych, W. Skomorowski, F. Pawłowski, R. Moszynski and Z. Idziaszek, 2010 *Phys. Rev. A* **83** 032723

[17] S Schmid, A. Härter, and J. H. Denschlag 2010 *Phys. Rev. Lett.* **105**, 133202

[18] H. J. Werner and P. J. Knowles 1985 *J. Chem. Phys.* **82** 5053

[19] P. J. Knowles and H. J. Werner 1985 *Chem. Phys. Lett.* **115** 259

[20] H. J. Werner and P. J. Knowles, 1988 *J. Chem. Phys.* **89** 5803

[21] P. J. Knowles and H. J. Werner 1985 *Chem. Phys. Lett.* **145** 514

[22] H. J. Werner and P. J. Knowles, F. R. Manby, M. Schütz, et al MOLPRO, version 2010.1, www.molpro.net

[23] Y. Wang and M. Dolg 1998 *Theor. Chem. Acc.* **100** 124

[24] L. von Szentpaly, P. Fuentealba, H. Preuss, and H. Stoll 1982 *Chem. Phys. Lett.* **93** 555

[25] P. Fuentealba, H. Stoll, L. v. Szentpaly, P. Schwerdtfeger, and H. Preuss 1983 *J. Phys. B* **16** L323

[26] E. R. Meyer and J. L. Bohn 2009 *Phys. Rev. A* **80** 042508

[27] J. Mitroy, M. S. Safronova and C. W. Clark 2010 *J. Phys. B: At. Mol. Opt. Phys.* **43** 202001.

[28] I. S. Lim, M. Pernpointner, M. Seth, J. K. Laerdahl, P. Schwerdtfeger, P. Neogrády, and M. Urban, 1999. *Phys. Rev. A* **60** 2822-2828.

[29] R. W. Molof, H. L. Schwartz, T. M. Miller, and B. Bederson 1974 *Phys. Rev. A* **10** 1131.

[30] R. J. Le Roy, Level 8.0: A Computer Program for Solving the Radial Schrödinger Equation for Bound and Quasibound Levels, University of Waterloo Chemical Physics Research Report CP-663 (2007); see <http://leroy.uwaterloo.ca/programs/>

[31] G. F. Gribakin and V. V. Flambaum 1993 *Phys. Rev. A* **48** 546

[32] V. V. Flambaum, G. F. Gribakin and C. Harabati 1999 *Phys. Rev. A* **59** 1998

[33] V. A. Dzuba and A. Derevianko 2010 *J. Phys. B*

43 074011
[34] Zhang P and Dalgarno A 2007 *J. Phys. Chem. A* **111** 12471
[35] X. Chu, A. Dalgarno and G. C. Groenenboom 2007 *Phys. Rev. A* **75** 032723
[36] A. Zangwill and P. Soven 1980 *Phys. Rev. A* **21**, 1561
[37] J. Mitroy and M. W. J. Bromley 2003 *Phys. Rev. A* **68** 052714